Proceedings of the 2004 IEEE
International Conference on Robotics & Automation
New Orleans, LA • April 2004

Design Issues in a Haptics-Based Master-Slave System for Minimally Invasive Surgery

M. Tavakoli, R.V. Patel and M. Moallem
Canadian Surgical Technologies & Advanced Robotics (CSTAR) and
Department of Electrical and Computer Engineering
University of Western Ontario, London, ON N6A 5B9, Canada
tavakoli@uwo.ca, rajni@eng.uwo.ca, mmoallem@engga.uwo.ca

Abstract— **Minimally invasive surgery (MIS) is an alternative to open surgery where special instruments are inserted into the body cavity through tiny incisions in order to perform surgical procedures. In this paper, some design issues in a master-slave robotic system for use in MIS are discussed. First, we discuss the design of a user interface that can be used to incorporate haptic interaction in robot-assisted MIS. Then we discuss the design of a laparoscopic end effector that meets MIS requirements and is instrumented for haptic feedback.**

I. Introduction

In minimally invasive surgery (MIS), the operation is performed using instruments designed to enter the body cavity through several tiny incisions of about 10 mm diameter while the surgeon monitors the procedure via a special camera (endoscope) inserted through one of the incisions. In the commercial robotic MIS systems, e.g. the ZEUS and the da Vinci surgical systems (from Intuitive Surgical Inc.), the surgeon's console provides visual feedback, but no force or torque information about the surgical field. It is known that incorporating force feedback into teleoperated systems can reduce the magnitude of contact forces and therefore the energy consumption, the task completion time and the number of errors. In various studies [1], [2], [3], addition of force feedback is reported to achieve some or all of the following: reduction of the RMS force by 30% to 60%, the peak force by a factor of 2 to 6, the task completion time by 30% and the error rate by 60%. Moreover, a force-reflective console for the surgeon can counterbalance the limited maneuverability of surgical instruments and restricted camera vision experienced in MIS.

Incorporating force feedback into a robotic MIS system calls for two devices: (a) a force-reflective user console, and (b) a surgical end-effector that can measure the tool/tissue interactions in the form of forces or torques. The haptic console can be used either in a master-slave setting or in a virtual-reality MIS simulation application. The reason for tool/tissue interaction measurements at the patient side is the superior performance and fidelity it can bring into haptics-based telesurgery, as opposed to *position-error based* haptic teleoperation [4].

In [5], a scenario is proposed to incorporate force feedback into the ZEUS surgical system by integrating a PHANToM haptic input device into the system. In [6], a telesurgery master-slave system that is capable of reflecting forces in three degrees of freedom (DOFs) is discussed. A 7-DOF haptic device that can be applied to surgical training is developed in [7]. A 5-DOF haptic mechanism that is used as part of a training simulator for urological operations is discussed in [8]. A slave system which uses a modified Impulse Engine (from Immersion Corp.) as the haptic master device is described in [9]. In [10], a dextrous slave combined with a modified PHANToM haptic master which is capable of haptic feedback in four DOFs is presented.

The layout of this paper is as follows: Parts II and III discuss the design and analysis of an interface with which the user controls an actual or virtual surgical manipulator and also feels the interactions occurring between the surgical tool and the tissue. Part IV discusses the development of a laparoscopic end-effector that is instrumented to measure the tool/tissue interactions at the slave.

II. Haptic Interface Architecture

Any MIS instrument enters the body through a tiny incision. Therefore the possible degrees of freedom are pitch, yaw, roll and insertion. The haptic user interface is configured to have the same degrees of freedom to provide a natural feel to the MIS surgeon.

A. Desirable Features and Human Factors for Haptic Interfaces

The desirable features of a haptic device [11] are as follows: (a) very little backdrive friction, (b) low inertia, (c) very little backlash in the transmission, and (d) capability for large force reflections. To correctly design a haptic device, the anatomical and physiological features of the human body, particularly the hand and fingers, must also be taken into account. First of all, a virtual surface with a stiffness of at least 20 N/cm or a resisting force of at least 11 N is perceived as solid and immovable by users [11]. This determines the maximum force that the device should be able to reflect. Secondly, human fingers can sense absolute and relative force variations of 0.5 N and $\pm 7\%$, respectively [1]. Therefore, for consistent force reflection, the interaction measurement at the surgical site as well as the haptic interaction at the user console should at least have this precision. For a detailed account of human factors in haptic devices, see [12].

B. Haptic Interaction in Pitch, Yaw and Insertion

The PHANToM 1.5A (Sensable Technologies Inc.) which provides force feedback in three translational degrees of freedom is integrated into the master interface. The PHANToM's stylus has been removed as it has only passive motions. A possible arrangement for the haptic interface is shown in Figure 1a. As part of the surgeon's console, a laparosopic instrument is passed through a fulcrum and then attached to the PHANToM end point. Therefore, the motions of the handles grasped by the surgeon are exactly the same as in conventional MIS. The instrument motions in pitch, yaw and insertion are registered by the PHANToM.

Force reflection is provided by the PHANToM in pitch, yaw, and insertion directions only. Roll and gripping are two motions

This research was supported by the Natural Sciences and Engineering Research Council (NSERC) of Canada under grants RGPIN-1345 and RGPIN-227612, and by the Ontario Research and Development Challenge Fund under grant 00-May-0709 and an infrastructure grant from the Canada Foundation for Innovation awarded to the London Health Sciences Centre (CSTAR).

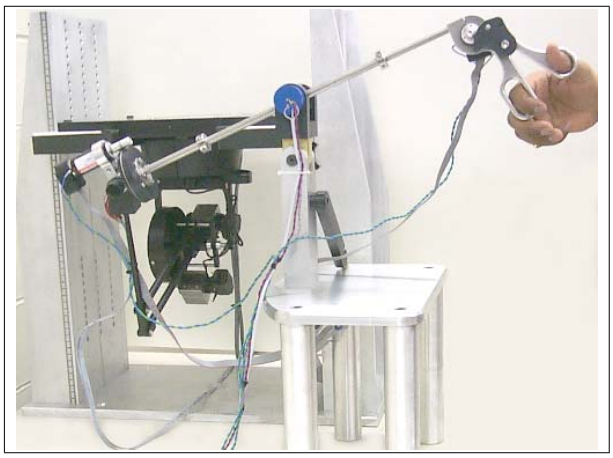

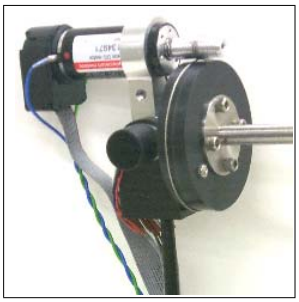

Fig. 1. (a) Master system and single-dof force reflection in (b) the finger loops (bottom left) and (c) the roll mechanism (bottom right)

which require additional actuation mechanisms for force reflection. We use a 1-dof haptic mechanism as described in the next section to establish force reflection in each of these directions.

The PHANToM can be oriented normally or upside down (as shown) and positioned in front of the fulcrum base or on its side (as shown), in order to optimize the instrument's workspace/manipulability and the user's dexterity/comfort.

C. Haptic Interaction in Roll and Gripping

A view of the 1-dof haptic mechanism for gripping is depicted in Figure 1b. Due to the requirement of large force reflections, use of a direct-drive motor is not an option. On the other hand, as studied earlier with regard to the PHANToM, gear reductions involve significant backlash while a cogless cable transmission (cable-capstan drive) can meet a simple low-friction zero-backlash reduction [11], [13]. Thus, in our 1-dof haptic device, a pre-tensioned cable pinned at both ends of the sector disk and wrapped several times around the motor pulley provides such a transmission. Here, the motor is secured to the fixed handle and through the cable transmission, rotates the other handle fixed to the sector disk. This can lead to application of forces against the squeezing thumb of the user. As shown in Figure 1c, a similar mechanism is also used for force reflection in the roll direction.

For haptic purposes, brushed DC motors are preferable over brushless motors which suffer from the reluctance cogging and torque ripple phenomena [13]. An appropriate brushed motor (Maxon Precision Motors) with a low inertia and low friction

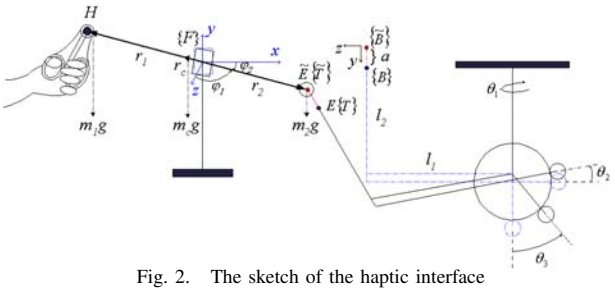

Fig. 2. The sketch of the haptic interface

is selected. To produce large forces, the stall torque for the motor is the primary specification. Given a desired range of motions, a desired maximum exertable force and a transmission ratio, the necessary peak torque for the motor was found from

$$\frac{F_{\max} \times (r_{\text{disk}} + L_{\text{handle}})}{\tau_{\text{stall}}} = \frac{r_{\text{disk}}}{r_{\text{mot}}} \tag{1}$$

III. Performance Analysis of the Haptic Interface

Here, we derive the Jacobian of the haptic interface and then analyze its performance.

A. Forward Kinematics and Jacobian

The PHANToM measures the position of its endpoint with respect to a fixed frame (called the base frame $\{B\}$) which coincides with its tool frame $\{T\}$ when the PHANToM is in the home position (zero position). The PHANToM is in home position when all control surfaces are at their right angle positions, i.e., when the arms and motors are at right angles to one another. For the PHANToM shown in Figure 2, the forward kinematics in the base frame are written as [14]:

$$\begin{aligned} x &= s_1(\ell_1 c_2 + \ell_2 s_3) \\ y &= \ell_2 - \ell_2 c_3 + \ell_1 s_2 \\ z &= -\ell_1 + c_1(\ell_1 c_2 + \ell_2 s_3) \end{aligned} \tag{2}$$

Therefore, the Jacobian of the PHANToM in the base frame is

$$J_{\text{PH}}(\theta) = \begin{pmatrix} c_1(\ell_1 c_2 + \ell_2 s_3) & -\ell_1 s_1 s_2 & \ell_2 s_1 c_3 \\ 0 & \ell_1 c_2 & \ell_2 s_3 \\ -s_1(\ell_1 c_2 + \ell_2 s_3) & -\ell_1 c_1 s_2 & \ell_2 c_1 c_3 \end{pmatrix} \tag{3}$$

Due to an attachment which connects the PHANToM's endpoint to the laparoscopic instrument endpoint, the length of the second arm of the PHANToM is increased to $\ell_2 + a$. Therefore, the position of the new endpoint $\tilde{E}$ with respect to the new base frame $\{\tilde{B}\}$ is found by replacing ℓ_2 by $\ell_2 + a$ in equations (2).

To find the position of the handle of the laparoscopic instrument H, we express all positions with respect to a fixed frame $\{F\}$ at the fulcrum. Here, d and β define the relative position and angle of the PHANToM with respect to the fulcrum base and L is the length of the laparoscopic instrument.

$$\begin{aligned} {}^{F}_{\tilde{B}}T &= \begin{pmatrix} \sin\beta & 0 & -\cos\beta & d \\ 0 & -1 & 0 & 0 \\ -\cos\beta & 0 & -\sin\beta & 0 \\ 0 & 0 & 0 & 1 \end{pmatrix} \\ {}^{F}X_{\tilde{E}} &= {}^{F}_{\tilde{B}}T\,{}^{\tilde{B}}X_{\tilde{E}} \\ {}^{F}X_{\tilde{H}} &= {}^{F}X_{\tilde{E}}\left(1 - \frac{L}{\|{}^{F}X_{\tilde{E}}\|_2}\right) \end{aligned} \tag{4}$$

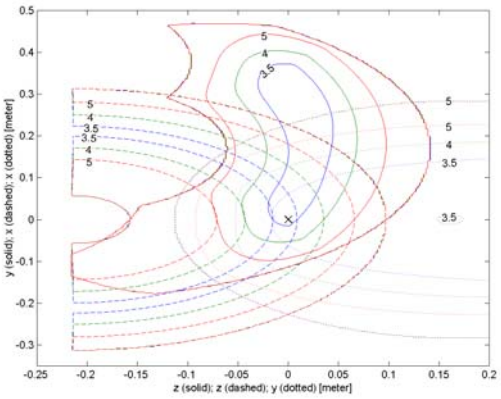

Fig. 3. Maximum normalized force feedback error (η) percentage per 1° angle offset (δ) at each point within the the workspace: $x = 0$ plane (solid), $y = 0$ plane (dashed) and $z = 0$ plane (dotted)

Using (4), the Jacobian of the haptic interface $J(\Theta, d, \beta)$ in frame $\{F\}$ is found where $\Theta = (\theta_1, \theta_2, \theta_3)$ is the PHANToM's motor position vector.

B. Sensitivity Analysis

A question that arises is the fidelity of the force feedback provided by the PHANToM. The issue is that the PHANToM's encoders measure positions relative to a fixed position (home position). The motor torque required to produce a force F at the end point is calculated as $F = (J_{\mathrm{PH}}^{\mathrm{T}}(\Theta))^{-1}\tau = J_F(\Theta)\tau$. Therefore, any offset from the zero position upon restart can cause erroneous θ_i measurements and consequently a deviation between the intended force and the actual force that is reflected to the user.

Assume that there is some small offset error δ in all encoder measurements, $\tilde{\theta}_i = \theta_i + \delta$, where $\tilde{\theta}_i$ and θ_i, $i = 1, 2, 3$, are the measured and true positions, respectively. The intended and actual force feedback at the end point are related to the motor torque vector τ as $\tilde{F} = J_F(\theta_i + \delta)\tau$ and $F = J_F(\theta_i)\tau$ respectively. We define the normalized force feedback error as

$$\eta = \frac{\|\tilde{F} - F\|_2}{\|F\|_2} = \frac{\|(J_F(\theta_i + \delta) - J_F(\theta_i))\tau\|_2}{\|J_F(\theta_i)\tau\|_2}$$

We would like to determine how the offset δ affects η. Since δ (rad) is small, a Taylor series expansion around θ_i yields:

$$J_F(\theta_i + \delta) \approx J_F(\theta_i) + \delta J^1(\theta_i)$$

Lemma 1: For any input p and output q related through a Jacobian relationship $q = \hat{J}p$, if $\|p\|_2 = 1$, then $\|q_{\min}\|_2 = \sigma_{\min}$ and $\|q_{\max}\|_2 = \sigma_{\max}$ where $\sigma_{\min}$ and $\sigma_{\max}$ are the smallest and largest singular values of the Jacobian matrix $\hat{J}$ [15].

Assuming, without loss of generality, that $\|\tau\|_2 = 1$, we get the following non-conservative bounds using Lemma 1:

$$\frac{\sigma_{\min}(J^1)}{\sigma_{\max}(J_F)} \leq \frac{\eta}{|\delta|} \leq \frac{\sigma_{\max}(J^1)}{\sigma_{\min}(J_F)}$$

Therefore, to have a normalized force feedback error $\eta \leq \eta_0$, enforces an upper bound on the initial angle error:

$$|\delta| \leq \eta_0 \min_{\text{workspace}} \frac{\sigma_{\max}(J_F)}{\sigma_{\min}(J^1)}$$

On the other hand, for some initial angle offset $\delta = \delta_0$, the normalized force feedback error is bounded at each point within the workspace as follows:

$$\eta \leq |\delta_0| \frac{\sigma_{\max}(J^1)}{\sigma_{\min}(J_F)} \tag{5}$$

Equation (5) is used to find the upper bound on η for $\delta = 1^\circ$ in $x = 0$, $y = 0$ and $z = 0$ planes (Figure 3). As is evident from the figure, we will have limited force feedback errors ($\eta < 10 - 15\%$) if $\delta < 3^\circ$. For this purpose, a hooking mechanism is devised in the haptic user console to hold the laparoscopic instrument level upon restart to ensure a small δ. Moreover, the parallelogram structure that exists in the PHANToM proves to be a great visual help to correctly place the PHANToM in its home position.

TABLE I

GCIs FOR TWO SETS OF JOINT ANGLE LIMITS AND ARM LENGTH RATIOS

Workspace boundaries	$\ell_2/\ell_1 = 0.79$	$\ell_2/\ell_1 = 0.96$
Normal orientation $\theta_{2_i} \in (-55^\circ, 90^\circ)$ $\theta_{3_i} \in (-40^\circ, 90^\circ)$	0.7679	0.7770
Upside down orientation $\theta_{2_i} \in (0^\circ, 90^\circ)$ $\theta_{3_i} \in (-40^\circ, 90^\circ)$	0.8154	0.8309

C. Workspace Analysis

Any haptic device control can be in the form of force control, position control or both. To improve the control accuracy for a manipulator, the Jacobian matrix condition number $\kappa = \|J\|\|J^{-1}\|$, where $\|J_{n\times n}\| = \sqrt{\mathrm{tr}(JJ^{\mathrm{T}}/n)}$, should be kept as small as possible at all points in the workspace. Instead of the Jacobian condition number, [16] introduces the global conditioning index (GCI) which concerns the overall conditioning of the manipulator across the workspace W rather than at each point therein:

$$\mathrm{GCI} = \frac{\int_W (\frac{1}{\kappa})\mathrm{dW}}{\int_W \mathrm{dW}} = \frac{\int_\Theta (\frac{1}{\kappa})|\det(J)|\mathrm{d}\theta_n \ldots \mathrm{d}\theta_1}{\int_\Theta |\det(J)|\mathrm{d}\theta_n \ldots \mathrm{d}\theta_1}$$

Larger values of GCI correspond to better conditioning. The above index has been maximized over the space of the manipulator DH parameters [16]. We would like, however, to use it as a quantitative measure for suitability of different subsets of the PHANToM's workspace. In particular, we are interested to see if the PHANToM should be oriented normally or upside down, in order to have a better conditioning index.

We would like the laparoscopic instrument to be levelled at the reset position with its end-point sweeping the space below that as the surgeon starts reaching the intended body part. We would also like the above reset position to be coincident with the PHANToM's home position in order to minimize the force reflection error (see section III-B). This simply means that the PHANToM has to be oriented upside down, with the laparoscopic instrument elevated in such a way that it is level when the PHANToM is in the home position. This selection of the PHANToM's orientation is also confirmed by Table I where the GCIs for normal and upside-down orientations of the PHANToM are compared. The GCI is lower for the normal orientation of the PHANToM where the motions of the laparoscopic instrument include $\theta_2 \in (-55^\circ, 0)$ into the workspace. Therefore, it is also better for control purposes to orient the PHANToM in an upside-down configuration. Table I also shows that the additional attachment that connects the PHANToM's end-point to the instrument end-point (thus increasing ℓ_2 by a) only helps to give a better

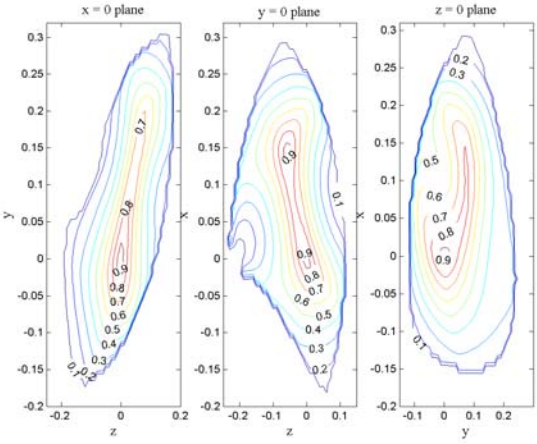

Fig. 4. Manipulability at each point within the workspace. Distances are in meters. Values are for $d = L/2$ and $\beta = 0$.

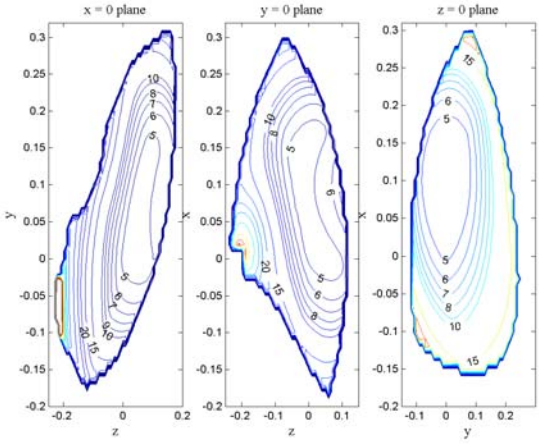

Fig. 5. Maximum force feedback for a unit torque at each point within the workspace. Distances are in meters. Values are for $d = L/2$ and $\beta = 0$.

conditioning index. This is because the GCI takes its maximum value for $\theta_{2_i} = 0$ and $\ell_2/\ell_1 = 1$ which is closest to the case when the PHANToM is upside down and the attachment exists.

For the configuration in Figure 1a, the workspace for the instrument covers a pitch angle of $\pm 30^\circ$ (up and down), a yaw angle of $\pm 40^\circ$ (side to side), a roll angle of $\pm 180^\circ$ (rotation about the instrument axis) and a displacement of ± 11 cm along the instrument axis. Also, the gripping handle angle ranges from 0 to 30°.

The manipulability $\mu = \sigma_{\min}(J)/\sigma_{\max}(J)$ of the haptic interface is shown in Figure 4. This is almost uniform in the neighborhood of the origin where the device is operated. Also note that the workspace is singularity-free.

D. Force Reflection Analysis

We would like to find out the maximum magnitude of forces that can be applied by a limited torque on the user's hand within the workspace. The motor torque and the resulting force F at the end point are related by $F = (J^{\mathrm{T}}(\Theta))^{-1}\tau = J_f(\Theta)\tau$ for any robot. For a unit torque vector ($\|\tau\|_2 = 1$), the limits on the magnitude of F are given as follows by Lemma 1:

$$\sigma_{\min}(J_f) \leq \|F\|_2 \leq \sigma_{\max}(J_f) \tag{6}$$

Using the Jacobian of the haptic interface $J(\Theta, d, \beta)$ given by (3) for $d = L/2$ and $\beta = 0^\circ$, the workspace map of the maximum force that can be exerted on the user's hand for a unit torque vector is shown in Figure 5. The lower bound on the maximum force is 5 N across the workspace. In the PHANToM where the stall torque[1] of each motor is 240×10^{-3} Nm and the capstan drive's transmission ratio is 11.6:1, the actual maximum force is about 2.8 times larger than what is shown in Figure 5. Also equation (1) gives the maximum exertable forces in the gripping and roll directions to be 17 N and 12 N respectively. These findings clearly meet our requirement on large force reflection as discussed in Section II-A.

E. Balancing

The haptic interface should be balanced so that the user does not feel any weight on his or her hand when no force is to be reflected. During the system design, the haptic mechanisms for the finger loops and the roll motion were intentionally placed on the two sides of the pivot point made by the fulcrum F, shown in Figure 2, such that we have as much balancing as possible. However, as the instrument moves through its workspace, further "active balancing" is required in the form of an additional force F_{B} exerted by the PHANToM's end-point on the instrument. Using the principle of virtual work:

$$W = (-m_1 g\hat{j})\mathrm{d}r_1 + (-m_2 g\hat{j} + F_{\mathrm{B}})\mathrm{d}r_2 + (-m_c g\hat{j})\mathrm{d}r_c = 0$$

where m_1, m_2 and m_c are the masses of the finger loops, the roll mechanism and the instrument shaft. Solving this equation for F_{B} results in

$$\begin{aligned} F_{\mathrm{B_x}} &= \frac{gT}{r_2}(-\sin^2\phi_1 \sin\phi_2 \cos\phi_2) \\ F_{\mathrm{B_y}} &= \frac{gT}{r_2}(\cos^2\phi_1 \cos^2\phi_2 \\ &- \cos^2\phi_1 - \cos^2\phi_2) + g(m_1 + m_2 + m_c) \\ F_{\mathrm{B_z}} &= \frac{gT}{r_2}(-\sin\phi_1 \cos\phi_1 \sin\phi_2) \end{aligned}$$

where $T = m_1 r_1 + m_1 r_2 + m_c r_2$ and r_1 and r_2 refer to the length of the corresponding vectors shown in Figure 2.

IV. Laparoscopic End-effector

Due to the incision size constraint in MIS, the diameter of the robotic end-effector including all force/torque measurement devices and the tool tip actuator is limited to 10 mm. This poses the following challenges: 1) Multi-axis force/torque sensors currently available are about twice as wide and therefore have to stay outside the patient, picking up unwanted abdominal wall friction and stiffness at the trocar site. 2) Due to the limited amount of space in MIS, the pivotal motions of the end-effector jaws (e.g. grasper jaws) need to be actuated by a linear motion. 3) For sterilizability reasons, it is desirable to use detachable tool tips that can be disposed of after use, so the sensor measuring the interactions between the tip and the tissue should not be mounted directly on the tip jaws.

Problem 1 can be tackled by non-invasive measurement of interactions using strain gauges placed on the laparoscopic end-effector. For problems 2 and 3, a mechanism consisting of a linear

[1] At maximum force (high stiffness resistance against the user's hand), the motor is almost steady.

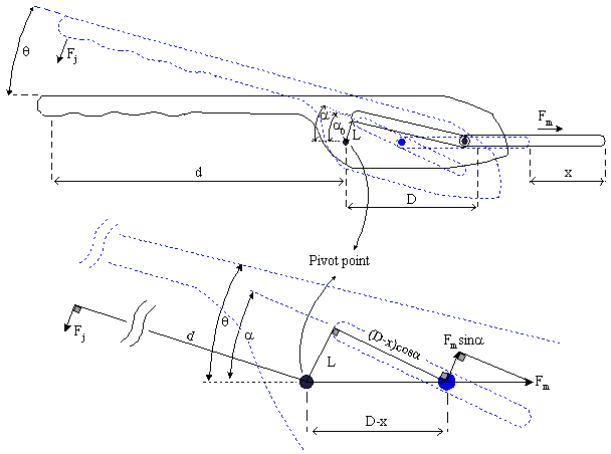

Fig. 6. Surgical grasper mechanism and a close-up

TABLE II
GRASPER TIP PARAMETER ESTIMATES

	α_0	L	D
Mean	25.15°	2.34 mm	5.91 mm
$\frac{\text{Std.dev.}}{\text{Mean}}$	2.1 %	3.9 %	1.7 %

motor and a load cell can be used to non-invasively actuate a detachable tip and measure its interactions with the tissue.

A. Surgical Tool Tip

The tools used in laparoscopic surgery to dissect, grasp, or cut tissue have their jaws pivotally moved relative to one another by a linear motion mechanism. To control the jaw position, it is necessary to find its relationship with the linear displacement. The sketch of an atraumatic forceps tip (Fundus grasper 3211, Microline Inc.) is shown in Figure 6. Here, $\alpha = \theta + \alpha_0$ and the jaw angle θ can be found from the linear motion as

$$\sin(\theta + \alpha_0) = \frac{L}{D - x} \tag{7}$$

The parameters α_0, L and D for this specific tool tip have to be found empirically. We set up an experiment in which a linear motor moves the tip to 30 positions (for the angle between the two jaws of the tip ranging from 0 to 63°) and registered the linear position x as well as the angle 2θ using a protractor. Then, a nonlinear minimization was carried out to find the values for α_0, L and D that best satisfy equation (7). The mean values for the resulting parameter estimates obtained using four experiments are listed in Table II. A consistency measure may be defined as the ratio of the standard deviation of the estimates to their mean value. Small consistency measures for the parameters estimated promise a good match with the actual values. The value of d is separately determined to be 22 mm.

Having obtained the position model of the tip, we need to find out the force model. According to Figure 6, the balance of moments about the pivot point leads to $F_j d = (F_m \sin\alpha)((D - x)\cos\alpha)$. Using equation (7) and $\alpha = \theta + \alpha_0$, the following force propagation model is found:

$$F_j = F_m \frac{L\cos(\theta + \alpha_0)}{d} \tag{8}$$

Therefore, it is possible to determine the tip interaction F_j based on the rod tension/compression F_m measurable by a single-axis load cell.

Fig. 7. From top to bottom and left to right: (a) twist motor and the end-effector assembly, (b) details of the end effector, (c) load cell to find tip forces, (d) gauges to measure bending moments, (e) gauges to measure the axial forces and (f) gauge to measure the torsional moment

It is important to appreciate the difference between the tip position (interaction) and the handle position (interaction) in a laparoscopic instrument. For example, in a Carl Storz Babcock grasper tool, there is a gain of 1.2 between the handle position and the tip position while the transfer function between the interaction (force or moment) at the handle and the tip is more involved [17]. In order to minimize the geometrical mappings that an MIS surgeon would have to learn to perform robot-assisted laparoscopic surgery, it is important to preserve the same tip/handle relationships in a telesurgery setting where the surgical end-effector's tip is controlled by a handle at the surgeon's console.

B. End-effector Assembly

Figure 7a shows the linear actuation assembly placed after a geared motor/encoder responsible for the twist motion. This assembly can be used with or without the free wrist (gimbals) made by the links L_1, L_2 and L_3. Without the wrist, the end-effector can be used with a robot (such as the da Vinci) that provides spherical movement at a Remote Center of Motion (RCM) located at the trocar (the incision point). Alternatively, the wrist can be used with any robot that provides positioning in 3-D space while a fulcrum placed next to the trocar forms a constrained isocenter and supports the end-effector so that its movements do not damage the tissue near the trocar. See [18] for a summary of surgical robotic systems and their characteristics including the number of DOFs and whether they provide an RCM.

It should be noted that the wrist is attached to the roll motor

TABLE III

VOLTAGE VS. AXIAL FORCE PARAMETER ESTIMATES

	Compression		Tension	
	α	β	α	β
Mean	2.58×10^{-1}	-7.09×10^{-1}	3.48×10^{-1}	-1.48×10^{-1}
$\frac{\text{Std.dev.}}{\text{Mean}}$	5.5%	8.1%	4.5%	31.8%

and is built such that if the motor faces resistance while trying to rotate the instrument body and the tissue grasped by it, the wrist will not twist into itself. This is simply because the axis of the motor and the axis of the joint connecting L_1 and L_2 are never aligned in the workspace ($-90^\circ <$ yaw angle $< 90^\circ$).

The parts of this assembly as well as two detachable scissors and grasper tips are shown in Figure 7b. There are three concentric tubes – outer, middle and inner. The inner tube is displaced with respect to the middle one by a linear motor (Zaber Technologies Inc.), in order to control the tip jaws. The reason for having an additional outer tube is to isolate the differential force exerted on the inner tube with respect to the middle one from force/torque measurements in other directions (see the next section).

C. Interaction Force/Torque Measurement

To measure the tip interaction force using equation (8), a load cell is attached between the linear motor shaft and the inner tube (Figure 7c). To find the forces $\begin{pmatrix} f_x & f_y & f_z \end{pmatrix}_{\text{tooltip}}$ and the twist moment τ_z due to tool-tissue interactions at the tip, it is sufficient to measure all moments $\begin{pmatrix} \tau_x & \tau_y & \tau_z \end{pmatrix}$ and one compressional/tensional axial force f_z. Here the assumption is that interactions only occur at the tool tip.

Most maneuvers involve lateral force interactions with the tissue at the instrument tip. We have put strain gauges on opposite sides of the surface of the outer tube such that any lateral force at the tip causes tension in one strain gauge and compression in the other (Figure 7d). These full-bridged gauges register the two bending moments τ_x and τ_y. Clearly, the middle tube which is made to float between the inner and outer tubes prevents the differential inner/middle tube force from affecting these gauges. Compressional/tensional axial forces which can occur when pushing or pulling on a tissue are registered by the full-bridged strain gauges placed on link L_3 of the 2-dof wrist (Figure 7e). The torsional moment, e.g., due to suturing, is measured by the torque gauge placed on the middle tube (Figure 7f) as the tip's outer body threads onto it. Note that each of the above strain gauges is in a transverse arrangement with respect to others and, therefore, is sensitive only in the intended direction.

We need to calibrate the strain gauges by finding the (linear) relationship between the output voltages and the forces/torques applied at the tool tip. For example, to calibrate the axial force gauge shown in Figure 7e, different masses are attached to the assembly held in the vertical direction and the voltage readouts are recorded. In this particular case, there is a no-load voltage present due to the weight of the motor. The least-squares method is used to find a line that best describes these data points in the voltage versus axial force plane. Table III shows the parameter estimates in $V = \alpha f + \beta$ where V is the voltage readout and f is the axial compression or tension force. Figure 8 shows the data points for the four experiments where the assembly has been under tension and the linear fit is as shown in Table 3. The calibration of the gauges responsible for measuring bending and torsional moments was done in a similar manner.

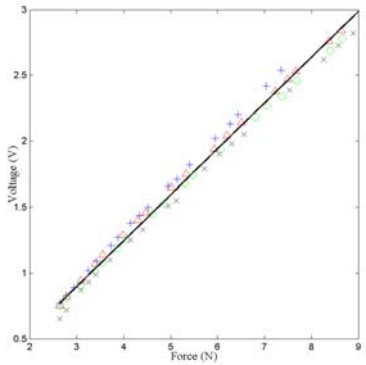

Fig. 8. The experimental $V - f$ data points (plus, cross, triangle, circle) and the least squares linear fit (solid line) during tension

REFERENCES

[1] K. B. Shimoga, "A survey of perceptual feedback issues in dextrous telemanipulation: Part I. Finger Force Feedback," in *Proc. IEEE Annual Virtual Reality Int. Symp*, Seattle, Washington, 1993.

[2] C. Wagner, N. Stylopoulos, and R. Howe, "Force feedback in surgery: Analysis of blunt dissection," in *The 10th Symp. on Haptic Interfaces for Virtual Environment and Teleoperator Systems*, Orlando, 2002.

[3] G. C. Burdea, *Force and Touch Feedback for Virtual Reality*. John Wiley & Sons, 1996.

[4] A. Sherman, M. Cavusoglu, and F. Tendick, "Comparison of teleoperator control architectures for palpation task," in *Proc. ASME Dynamic Systems and Control Division*, S. S. Nair, Ed., vol. DSC 69-2, 2000, pp. 1261–8.

[5] T. Ortmaier, D. Reintsema, U. Seibold, U. Hagn, and G. Hirzinger, "The DLR minimally invasive robotics surgery scenario," March 2001, workshop on Advances in Interactive Multimodal Telepresence Systems, Munich, Germany.

[6] M. Ottensmeyer, "Telerobotic surgery – feedback time delay effects on task assignment," Master's thesis, MIT, Cambridge, MA, 1996.

[7] V. Hayward, P. Gregorio, O. Astley, S. Greenish, and M. Doyon, "Freedom-7: A high fidelity seven axis haptic device with application to surgical training," Experimental Robotics, Lecture Notes in Control and Information Science 232, Springer Verlag, 1998.

[8] K. Vlachos, E. Papadopoulos, and D. Mitropoulos, "Design and implementation of a haptic device for training in urological operations," *IEEE Transactions on Robotics and Automation*, vol. 19, pp. 801–808, 2003.

[9] M. C. Cavusoglu, F. Tendick, M. Cohn, and S. S. Sastry, "A laparoscopic telesurgical workstation," *IEEE Transactions on Robotics and Automation*, vol. 15, pp. 728–739, 1999.

[10] A. Madhani, G. Niemeyer, and K. S. Jr., "The black falcon – a teleoperated surgical instrument for minimally invasive surgery," in *IEEE/RSJ International Conference on Intelligent Robots and Systems*, Victoria, BC, Canada, 1998.

[11] T. H. Massie, "*Design of a Three Degree of Freedom Force-Reflecting Haptic Interface*," B.S. thesis, MIT, May 1993.

[12] C. Youngblut, R. E. Johnston, S. H. Nash, R. A. Wienclaw, and C. A. Will, "Review of virtual environment interface technology," Institute for Defense Analyses (IDA) Paper P-3186, 1996.

[13] M. Arcy, "Design of a single degree of freedom mechanical breadboard haptic display," Master's thesis, Northwestern University, Evanston, IL, 1996.

[14] M. C. Cavusoglu and D. Feygin, "A critical study of the mechanical and electrical properties of PHANToM haptic interface and improvements for high performance control," *Presence: Teleoperators and Virtual Environments*, 2002.

[15] F. Gao and W. A. Gruver, "Performance evaluation criteria for analysis and design of robotic mechanisms," in *The 8th International Conference on Advanced Robotics*, Monterey, CA, 1997.

[16] C. Gosselin and J. Angeles, "A global performance index for the kinematic optimization of robotic manipulators," *Transactions of the ASME, Journal of Mechanical Design*, vol. 113, pp. 220–226, 1991.

[17] J. Rosen, B. Hannaford, M. MacFarlane, and M. Sinanan, "Force controlled and teleoperated endoscopic grasper for minimally invasive surgery - experimental performance evaluation," *IEEE Transactions on Biomedical Engineering*, vol. 46, pp. 1212–1221, 1999.

[18] R. H. Taylor and D. Stoianovici, "Medical robotics in computer-integrated surgery," *IEEE Transactions on Robotics and Automation*, vol. 19, pp. 765–781, 2003.